

Title: Limit 75 characters

Multi-Site Optical Monitoring of Spinal Cord Ischemia During Spine Distraction

Running Title: Limit 45 characters

Multi-site Optical Monitor of Spinal Ischemia

David R. Busch PhD, Wei Lin PhD, Chunyu (Hunter) Cai MD, PhD, Alissa Cutrone BS, Jakub
Tatka MD, Brandon J. Kovarovic MEng, Arjun G. Yodh PhD, Thomas F. Floyd MD, James

Barsi MD

D. R. Busch, Ph.D, Assistant Professor

5353 Harry Hines Blvd

Department of Anesthesiology and Pain Management

Department of Neurology and Neurotherapeutics

University of Texas Southwestern, Dallas, TX, USA

75201-9068

214-648-8232

David.Busch@UTSW.edu

W. Lin, Ph.D., Associate Professor

100 Nicolls Rd.

Department of Biomedical Engineering, Stony Brook University, Stony Brook, NY, USA

11794-5281

631-632-1639

Wei.Lin@stonybrook.edu

C. Cai, M.D. Ph.D, Assistant Professor

5353 Harry Hines Blvd

Department of Pathology, University of Texas Southwestern, Dallas, TX, USA

75390-9072

214-648-2327

Chunyu.Cai@UTSouthwestern.edu

A. Cutrone, B.S. Research Assistant

Department of Cell and Developmental Biology, Vanderbilt University, Nashville, TN, USA

2601A Blakemore Avenue

Nashville, TN 37212

631-972-8167

alissa.m.cutrone@vanderbilt.edu

J. Tatka, M.D., Assistant Professor

Department of Orthopedic Surgery, Columbia University Medical Center, New York, NY,
USA

55 Palmer Ave

Bronxville, NY 10708

914-787-5175

jt3129@cumc.columbia.edu

B. J. Kovarovic, M.Eng, Research Assistant

T8-050 Health Sciences Center,

Stony Brook, NY, 11794-8084

(914) 703-2649

brandon.kovarovic@stonybrook.edu

A. G. Yodh, Ph.D. Professor

3231 Walnut St.

Department of Physics and Astronomy, University of Pennsylvania, Philadelphia, PA, USA

19104

[215-898-8571](tel:215-898-8571)

yodh@physics.upenn.edu

T. F. Floyd, M.D. Professor
5353 Harry Hines Blvd
Department of Anesthesiology and Pain Management
Department of Cardiovascular and Thoracic Surgery
Department of Radiology, University of Texas Southwestern, Dallas, TX, USA
75201-9068
214-648-8235
Thomas.floyd@utsw.edu
(Corresponding, and co-senior author)

J. Barsi, M.D. Assistant Professor
14 Technology Drive
Department of Orthopedic Surgery
Stony Brook University, Stony Brook, NY, USA11733
631-444-4233
james.barsi@stonybrookmedicine.edu

This study was supported by the DePuy Synthes Spine Research Grant from the Pediatric Orthopaedic Society of North America (PI JB, TFF) and the Craig H. Neilsen Foundation Senior Research Grant (PI TFF, AGY). During the study, several authors received support from the NIH (AGY, WL, DRB). Funders were not involved in the design, analysis, or interpretation of the study.

Dr. Barsi has received personal fees from K2M, outside the submitted work.

Several authors have patents issued (US20140343384 (AGY, TFF), US8,082,015 (AGY), US6,076,010 (AGY), US10,342,488 (AGY, DRB) or pending PCT/US2015/017286 (AGY, DRB). None of these patents are licensed or generate royalties.

Dr. Floyd is the CEO and President of NFOSYS, Inc. This company may license the technology used in this study. There is currently no license and no sales.

Dr. Tatka, Dr. Cai, Mr. Kovarovic and Ms. Cutrone have nothing to disclose.

Keywords

Spinal cord, blood flow, trauma, surgery, monitoring, injury

Abstract

Optimal surgical management of spine trauma will restore blood flow to the ischemic spinal cord. However, spine stabilization may also further exacerbate injury by inducing ischemia. Current electrophysiological technology is not capable of detecting acute changes in spinal cord blood flow or localizing ischemia. Furthermore, alerts are delayed and unreliable. We developed an epidural optical device capable of directly measuring and immediately detecting changes in spinal cord blood flow using diffuse correlation spectroscopy (DCS). Herein we test the hypothesis that our device can continuously monitor blood flow during spine distraction. Additionally, we demonstrate the ability of our device to monitor multiple sites along the spinal cord and axially resolve changes in spinal cord blood flow.

DCS-measured blood flow in the spinal cord was monitored at up to three spatial locations (cranial to, at, and caudal to the distraction site) during surgical distraction in a sheep model. Distraction was halted at 50% of baseline blood flow at the distraction site. We were able to monitor blood flow with DCS in multiple regions of the spinal cord simultaneously at ~ 1 Hz. The distraction site had a greater decrement in flow than sites caudal to the injury (median -40 vs. -9%).

This pilot study demonstrated high temporal resolution and the capacity to axially resolve changes in spinal cord blood flow at and remote from the site of distraction. These early results suggest that this technology may assist in the surgical management of spine trauma and in corrective surgery of the spine.

Introduction

Spinal cord blood flow and regulation is impaired after traumatic spinal cord injury¹ and low spinal cord perfusion pressure predicts poor outcome.² Hypotension, hypoxia, vasospasm, inflammation, edema, and hemorrhage all propagate spinal ischemia after injury.³ From the limited information available from animal research, it is thought that decompression and stabilization after injury may significantly improve spinal cord hemodynamics.^{4,5} Conversely, it is also possible that stabilization and decompression for trauma may worsen spinal cord blood flow, as spinal cord ischemia complicates even elective spine surgery.⁶⁻⁸

Distraction-related neurologic injury is thought to occur from (1) vascular compromise from stretching leading to ischemia;^{4,5,9} and (2) direct traction disrupting the spinal cord tracts.¹⁰ A study of animal models suggests that vascular compromise temporally precedes direct injury; therefore, the ability to monitor blood flow during distraction may enable earlier intervention before the onset of a traction injury.^{4,7,11}

With continuous evoked potential monitoring, the neurologic function of the spinal cord can be assessed during surgical correction and has become the standard of care in performing spine surgery.¹² Somatosensory-evoked potentials and motor-evoked potentials (MEPs) monitor the integrity of the posterior spinal sensory pathways and the anterior and lateral spinal motor tracts, respectively. However, signals are often delayed relative to the inciting event, limiting the efficacy of any intervention to preserve function. Delays of 7 to 19 minutes in the response of somatosensory-evoked potentials and 11 to 17 minutes in the response of MEPs have been reported after the onset of purely ischemic interventions.^{13,14} Evoked potential monitoring may also be influenced by other factors including anesthesia, temperature, and limb perfusion.^{15,16} A 2012 evidence-based clinical guideline found that only 16% to 40% of patients with substantial electrophysiologic changes intraoperatively had postoperative-onset paraparesis, paraplegia, or quadriplegia.¹⁷ Nevertheless, although this method is flawed, no clinically viable technique currently exists to directly evaluate spinal cord perfusion and enable surgeons to preserve function.

As ischemia, secondary to stretching and vasospasm of the vasculature appears to precede any mechanical axonal disruption of the cord, a monitor designed to monitor blood would seem to offer the earliest alert of impending injury. The most frequently used technology is laser Doppler flowmetry (LDF),¹⁸⁻²⁰ which measures flow in a very limited tissue volume, 0.3-0.5 mm³, in close proximity to the probe tip and at single spinal level (spatial position). Unless the LDF probe is placed to penetrate the spinal cord, it can only measure superficial tissue. Additionally, positioning of the rigid probe is troublesome, the probes are prone to movement and fracture, and they cannot be left in place for an extended period of time. Use of laser speckle contrast imaging (LSCI) to measure spinal cord perfusion has been reported.¹ However, like LDF, this technique is sensitive only to superficial blood flow and therefore typical implementations of technique using a camera require exposure of the measured regions of the spinal cord to the illumination and detection optics, i.e., a large laminectomy. Additionally, blood on the dural surface can interfere with this measurement.

Near-infrared (NIR, ~650-950nm) light is highly scattered, but minimally absorbed, in most tissues.²¹ Thus, NIR photons travel for long distances in tissue, permitting NIR light to measure 'deep' tissues (>1cm below the illuminated surface) with multiply scattered light. Diffuse correlation spectroscopy (DCS) is a recently developed optical monitoring technique that uses long coherence-length NIR lasers to illuminate tissue and detect fluctuations in the interference pattern of light that has propagated through tissue.^{22, 23} DCS has rigorous mathematical underpinnings²³ and has been validated as a way to measure blood perfusion,²⁴⁻²⁸ including in the ischemic ovine spinal cord,^{29, 30} which is similar in size and physiology to the human spinal cord.³¹ Briefly, DCS relies upon the temporal fluctuations in the intensity of a single light speckle or spatial mode provide insight into the motion of blood cells. These fluctuations are readily quantified by the intensity temporal autocorrelation function of transmitted light. The resultant data may be fit to a photon diffusion (correlation diffusion) model to determine a blood flow index (BFI).

The novel technology that we apply in this pilot study does not require laminectomy, preserving the interaction of the lamina/ligaments upon spinal cord blood flow.

Measurements also reflect interrogation of the entire depth of the cord without injuring the cord. Data can be obtained continuously and we can monitor multiple injured and non-injured sites simultaneously.

Materials and Methods

All animal studies were approved by the Institutional Animal Care and Use Committee of Stony Brook University under protocol 404982-2, originally approved 2012. The experimental facilities are certified by the American Association for the Accreditation of Laboratory Animal Care.

Experimental Overview

We utilized a thin, highly flexible fiber optic probe employing Diffuse Correlation Spectroscopy (DCS) to test the ability of the device to measure spinal cord blood flow at the site of gradually increasing spinal distraction. Distraction was halted when the blood flow reached 50% of baseline. Additionally, in a subset of animals, we monitored blood flow cranial or both cranial and caudal to the site of distraction to test the ability of the device to detect regional changes in blood flow, i.e., axially resolving the location of ischemia along the spine. Finally, in another subset of animals, we successfully utilized motor evoked potential (MEP) monitoring during spinal cord distraction. Animals were recovered overnight. On the morning after surgery, animals underwent a neurobehavioral assessment, were euthanized, and immediately thereafter spinal cords were harvested for histopathological analysis.

The Sheep Model and Sample Size Justification

Experiments were performed in a Dorsett sheep model. The sheep spine is similar in size and physiologic properties to that of humans.³¹ The sheep model has been used extensively for research using similar devices, such as cerebrospinal catheters, spinal stimulators, epidural catheters, and both endovascular and open vascular aortic interventions.³²⁻³⁵

Ten healthy male and female Dorset sheep 2 to 3 years old weighing approximately 65 kg were used for the study. Our a priori sample size calculation suggested that eight sheep would be necessary to identify a difference in blood flow at the site of distraction of 50%

(power of 0.8; significance 0.05), assuming a 25% standard deviation. A priori sample sizes were not calculated based upon secondary neurobehavioral or neurohistopathological outcomes. Animals were housed in individual, adjacent stalls permitting interaction as well as monitoring of individual water and food consumption, per local veterinary policy. Surgeries began at 8:00 am local time.

Surgical Procedures

Animals were pre-treated with glycopyrrolate (0.02 mg/kg, intramuscular) in their pens before transport to the surgical suite. Anesthesia was induced with ketamine (10–20 mg/kg intramuscular). After this step, an intravenous catheter was placed to permit use of intravenous agents and to deepen the anesthetic for intubation. Femoral artery and central jugular intravenous cannula were placed after anesthetic induction to continuously measure the mean arterial pressure (MAP) and provide intravenous infusions of anesthesia. Animals were maintained on isoflurane 2.0% to 3.5% during surgical exposure, supplemented with fentanyl (5–10 µg/kg/hr) and rocuronium (0.3–1.25 mg/kg).

After the spine was exposed, isoflurane was discontinued, rocuronium was reversed with neostigmine (0.7 mg/kg). During spine distraction an appropriate plane of anesthesia was maintained with a propofol infusion (100–30,000 µg/kg/min intravenously) supplemented with fentanyl (5–10 µg/kg intravenously) and ketamine as-needed boluses (1–5 mg/kg intravenously) in response to any movement.

Prior to surgery, animals were positioned prone on a radiolucent midline chest support device on a fluoroscopy table, then covered and warmed with a Bair Hugger (3M, Maplewood, MN, USA) forced-air heating blanket with a portal for surgical access. Temperature was monitored via a rectal thermistor. After fluoroscopic identification of the appropriate spine level, a midline incision was made down to the spinous processes. Electrocautery was used for subperiosteal dissection to the tips of the transverse processes. Pedicle start points were identified using anatomic landmarks and confirmed using fluoroscopy. A burr was used to make a pilot hole, and a pedicle awl was used to create a tract down the pedicle into the vertebral body. A ball-tipped probe was used to palpate the tract and confirm the position was acceptable. The tract was tapped and an

appropriately sized stainless-steel poly-axial pedicle screw (K2M, Leesburg, VA, USA) was placed. Screws were placed bilaterally in sequential vertebrae between the T9 and L1 levels. A 5.5-mm stainless steel rod was placed in the head of the pedicle screw. Proximal endcaps were fully tightened and distal endcaps were loosely applied, permitting motion along the rod during the distraction maneuver.

After placement of instrumentation, a laminotomy was created at least three levels caudal to the instrumented level; this separation distance minimizes artifacts associated with the laminotomy. DCS fiber optic probes were placed through this laminotomy into the epidural space and advanced under fluoroscopic imaging at the level of distraction (Sheep 1, 2), additionally at two levels cranial to the distraction site (Sheep 3 to 10), and one or two levels caudal to the site of distraction (Sheep 4, 9, 10). Specifics of probe placement for each sheep are described below.

DCS flow was continuously monitored (described below) throughout distraction, which was performed in intervals of 2 mm by placing ratcheting distractors bilaterally between the pedicle screws. After each distraction step, screw endcaps were tightened to maintain distraction, and the animal was monitored for 2 minutes. When measured, bilateral MEPs were acquired at the end of each 2-minute interval. A Vernier caliper was used to confirm the length of distraction by measuring the distance between the pedicle screws bilaterally. Distraction was terminated when either a 50% fall in blood flow was measured with DCS (that is, $\Delta\text{BF} = -50\%$) or when the maximum range of the ratchetting distractor was reached. After completion of the monitoring protocol, the distraction was released to allow the spine to relax. The hardware was removed and the wound was closed; monitoring continued throughout this period. Postoperative pain was managed with buprenorphine 0.05 mg/kg to 0.01 mg/kg every 8 hours, and a fentanyl patch (2-3 $\mu\text{g}/\text{kg}/\text{hr}$) was sutured subdermally at the conclusion of surgery. This was supplemented with carprofen 2 mg/kg to 4 mg/kg subcutaneously and morphine sulfate 0.1-0.2 mg/kg every 6 hours as needed.

Monitoring

MEP monitoring was conducted using a Nihon Kohden Neuropack MEB-9400 S1 (Nihon Kohden America, Irvine, CA, USA). Disposable subdermal needle electrodes were placed according to the International 10-20 system. The motor stimulus electrodes were placed a few centimeters behind the Cz plane at C3' to C4'. The motor recording electrodes were placed in semi-membranous tissues or the gastrocnemius muscles in the lower extremities and in the flexor carpi ulnaris for the upper limbs. The paradigm of motor cortex transcranial stimulation used a train of five pulses with a duration of 0.05 ms, an inter-stimulus interval of 2 ms, and a voltage adjusted between 100 and 500 volts to produce a compound muscle action potential $\geq 50 \mu\text{V}$.

The optical probes used in this study consisted of a flexible sheath 0.9 mm in diameter enclosing a pair of single-mode detector fibers and a source fiber (Fiberoptic Systems Inc, Simi CA, Fig. 1). The tip of each fiber was polished at a 45° angle to direct the light perpendicular to the axis of the probe. The detector fiber tips were positioned 2 cm axially from the source fiber tip and provide redundancy at each probe location. Up to three of these probes were inserted through a single laminotomy.

DCS was monitored continuously throughout distraction and recovery. BFI values were derived from DCS data fit to a semi-infinite photon diffusion model using a field-programmable gate-array analysis device at 0.5 Hz to 2 Hz, depending on the integration time necessary to achieve an acceptable signal-to-noise ratio.³⁶ The BFI was normalized to the pre-intervention baseline (after installation of surgical hardware), producing a change in the relative BFI ($\Delta\text{BF} = [\text{BFI} / \text{BFI}_0 - 1] * 100$) that was displayed in real time. After reaching $\Delta\text{BF} = -50\%$ or the maximum range of the ratchetting distractor, DCS was monitored continuously for 10 minutes; if performed, MEP were measured every 2 minutes. In post-processing, the difference in the nadir of blood flow at injured and non-injured locations was assessed with Wilcoxon's rank sum test.

Assessment of Neurological Deficits

We assessed the functional deficit created by spinal distraction using a modified Tarlov scale 24 hours postoperatively.^{37,38} Focusing on the hindlimb, this scale ranges from 0 (no voluntary movement) to 6 (normal movement):

Tarlov 0: No voluntary movement

Tarlov 1: Barely perceptible movement

Tarlov 2: Brisk movement, but no weight support or coordination

Tarlov 3: Alternate stepping and movement

Tarlov 4: Weight support

Tarlov 5: Ambulation with mild deficit

Tarlov 6: Normal movement.

Histology

Immediately after the functional assessment, animals were euthanized, and the spinal cord was harvested for histopathological analysis. Sections of spinal cord (2 cm) were excised at the site of distraction and at the caudal- and cranial-to-injury DCS monitoring sites. These sections were fixed in 10% formalin before being embedded in paraffin. Subsequently, six cross-sections, 5- μ m thick, were recovered from each spinal cord section. To assess an acute axonal injury in the spinal cord, we used beta amyloid precursor protein (β -APP) immunohistochemistry. β -APP is a membrane protein synthesized in the cell body of neurons and transported to the synapses by fast anterograde axoplasm transport.³⁹ Acute axon injury impedes axonal transport, leading to local accumulation of β -APP and axonal spheroid formation at the proximal stump at the site of the injury.⁴⁰ β -APP immunostaining enables the detection of axonal injury within hours of the injury,⁴¹ although β -APP expression alone does not differentiate axonal injury from mechanic force, hypoxia, or other causes.⁴²

For β -APP detection, immunohistochemistry of β -APP (Millipore, Catalog MAB348, Clone: 22C11; Dilution 1:20000) was performed on 5- μ m-thick paraffin sections in a Clinical

Laboratory Improvement Amendment (CLIA) approved laboratory on a Leica Bond-III automated immunostainer using Fast Red chromogens from Bond Polymer Refine Detection kits (Leica Microsystems, Buffalo Grove, IL, USA, DS9390) as red secondary stains to detect signals. Adjacent sections stained with hematoxylin and eosin were examined for comparison with the immunohistochemistry slides.

The β -APP immunohistochemistry slides were interpreted by a board-certified neuropathologist (CC), who was blinded to the site of distraction, changes in blood flow, and the animals' postoperative Tarlov scales. The extent of axonal injury was quantified under a light microscope as an β -APP score. The β -APP score was determined by manually counting the number of β -APP-positive axonal spheroids with diameter $>10\mu\text{m}$ in a 40x high-powered field (HPF), in the region of the highest spheroid density (Fig. 2). Spinal cord injury was considered none (0 spheroids/HPF), mild (1-9 spheroids/HPF), moderate (10-50 spheroids/HPF), and severe (>50 spheroids/HPF, or the presence of cavitory lesion, hemorrhage or confluent β -APP staining). For each animal, 3-5 sections of spinal cord at, above or below the level of the site of injury were examined in a blind fashion. The resulting β -APP score was compared with the score for other experimental metrics.

Primary and Secondary Measurements

In this pilot study, our primary goal was to test the ability of DCS to monitor blood flow continuously at the site of gradually increasing distraction, comparing these continuous measurements to baseline (pre-distraction) measurements. Additionally, we compared changes in blood flow at the distraction site to changes in blood flow in cranial and caudal sites. We also compared reductions in blood flow at the site of distraction to the occurrence of axonal injury by comparing β -APP scores from histological samples at, cranial to, and caudal to the distraction point. Finally, we compared time courses of changes in spinal cord blood flow at the site of injury with changes in MEP amplitudes.

Results

Table 1 summarizes the maximum distraction distances and minimum blood flow at each probe position (measurements from the same probe were averaged together). In our sample of 13 sheep, three were excluded from the analysis because of surgical

complications leading to breakage of the optical probe (one animal) and inability to reliably radiographically visualize the probe location relative to the site of distraction (two animals). One sheep died while recovering from anesthesia (Sheep 1); this sheep was not included in the neurobehavioral or histopathological assessment.

DCS blood flow index (BFI) was continuously monitored at the distraction site in 10 sheep; and was significantly lower than baseline in the ten minutes after maximal distraction (pre-distraction baseline: $\Delta\text{BF} = 0$; maximum distraction: median $\Delta\text{BF} = -40\%$, interquartile range [-43, -26]; Fig. 3A). Moreover, in 8 sheep measured at multiple sites, blood flow at the distraction site was reduced at maximal distraction compared to sites cranial to the injury ($\Delta\text{BF} = -7\%$; [-12, 13]; $p < 0.001$). The caudal site was not significantly different from the distraction site ($\Delta\text{BF} = -7\%$ [-25%, -1%]; $p = 0.11$). After release, blood flow at the distraction site recovered to a median ΔBF of -13% [-31%, -5%].

Fig. 4 shows an example of continuous measurement of blood flow at and cranial to the distraction site throughout distraction and release in a single sheep. Blood flow cranial to the distraction site was fairly stable (less than 20% variation) during the distraction procedure. By contrast, blood flow at the distraction site was depressed during distraction, recovering to near baseline after release of mechanical traction.

At the site of injury, β -APP score was (median [IQR], higher is worse) 38 [5, 64]; caudal to the site of injury β -APP score was 15 [4, 34]; cranial to the injury β -APP score was 0 [0, 1]. These data are shown graphically in Fig. 3B; statistical significance between groups was calculated using the Wilcoxon Rank Sum test. The β -APP score cranial to the site of injury was lower than the distraction site (trending towards significance, $p = 0.051$) while the score caudal to the site of injury was not significantly different.

Adequate-quality serial MEP signals could only be obtained in four of 10 sheep, likely because of the skull's thickness over the motor cortex. The median [IQR] fractional change in the MEP amplitude, immediately after achieving $\Delta\text{BF} = -50\%$, was -15% [-53%, 11%] (full range -89% to 34%). Prior to release of distraction in these four sheep, approximately 10 minutes later, the change in MEP amplitude from baseline ranged from -91% to 46%, with a median of -87%.

We present the contrasting results of two of those studies in which MEP and DCS data were acquired. In Fig. 5 and Fig. 6, the time courses of the percentage of change in blood flow from baseline, distraction distance, and amplitude of evoked potential are shown. In Fig. 5 changes in MEP amplitude in lagged changes in DCS blood flow during distraction. In Fig. 6, changes in MEP amplitude more closely followed change in blood flow during distraction.

Tarlov scores were correlated with β -APP scores (Spearman's rho, $\rho = -0.76$; $p = 0.026$); blood flow changes at the injury site and the maximum distraction distance were not correlated with either the Tarlov score or β -APP score.

Discussion

Ischemia is an important mechanism of injury to the spinal cord during trauma and spine surgery for the correction of traumatic, congenital, and acquired deformities. Current intraoperative methods to monitor ischemia have known delays in detection and only indirectly measure ischemia through changes in electrophysiological signals. There is no clinical tool that allows for the continuous and direct measurement of spinal cord blood flow intra-operatively at a single site, much less at multiple sites. This pilot study demonstrates the ability of a fiber optic device, employing diffuse correlation spectroscopy (DCS), to measure blood flow continuously at multiple sites throughout spine distraction, in a large animal model.

Unlike evoked potential monitoring, which reports on the functionality of the entire nerve pathway, the DCS device allows for the axial localization of changes in blood flow within the spinal cord. We found that the DCS measured blood flow index decreased most at the site of distraction ($\Delta BF = -40\%$) compared to cranial to the distraction site ($\Delta BF = -7\%$; $p < 0.01$). Blood supply to the spinal cord is complex consisting of three longitudinal arteries descending from the vertebral arteries and multiple segmental medullary arteries entering along its length. Blood flow cranial to the site of distraction may be less affected by an injury to the spinal vasculature at the site of distraction. All sites measured had lower average flow during distraction. It is possible that changes in blood flow extend over several spinal levels and not just at the distraction site as has been reported in the

literature.⁹ It is unclear the exact distance from the site of distraction that this effect is seen. A future study measuring blood flow at defined intervals from the distraction site will better characterize this effect.

After release of the distraction, blood flow at the site increased but was still lower than at baseline ($\Delta\text{BF} = -13\%$). We acknowledge that this measurement is susceptible to motion artifact from abrupt movement of the vertebrae when distraction is released; moreover, the vertebrae did not always relax to their pre-distraction position. Nevertheless, this observation suggests that ischemia may persist despite complete removal of the distraction force. This finding of decreased blood flow at the site of distraction is similar to the findings of Naito⁵ and Owen⁹ who used a hydrogen wash out technique to assess blood flow. A larger sample with additional measurement sites along the length of the spinal cord may be better able to differentiate these factors.

In this small sample, our histologic findings were consistent with localized injury at the site of distraction ($\beta\text{-APP} > 35$ in 6 of 9 samples) and disruption of the cranial to caudal vessels; however, this trend was not statistically significant. The median greatest degree of injury found on the histopathology and the greatest decrement in blood flow were both at the site of distraction. Injury may have been limited by our protocol in which distraction was halted when blood flow decreased to 50% of baseline, suggesting potential studies into the benefit of blood flow monitoring to guide early intervention and prevention of more extensive injury. As expected, the maximum $\beta\text{-APP}$ score was correlated with motor deficits measured with the modified Tarlov scale. Reductions in blood flow alone, as measured by DCS, were not associated with motor deficits, although this may have been a function of insufficient sample size. Likewise, with MEP measurements in only four sheep, we could not statistically correlate DCS with MEP; however, our preliminary findings on that comparison were intriguing. Ischemia may be the earliest contributor to SCI during a distraction injury, and its early identification may prevent subsequent physical disruption of the spinal cord.

Our histologic findings suggest that the MEP changes were not related to physical disruption of the axons and were therefore related to ischemia. While MEP data was only

able to be acquired in four animals, our results demonstrated an important temporal insensitivity in the MEP amplitude relative to blood flow changes as measured with DCS. At the time point which $\Delta\text{BF} = -50\%$, MEP was noted to be decreased by only $\sim 15\%$. At ten minutes at this level of distraction, MEP declined by 87%. This is similar to the findings of Hong,⁴³ who found a delayed spinal cord injury of 10.7 minutes at a mean of 20.9 mm distraction in a porcine model. Similarly, Lips has shown there is a delayed detection of motor pathway function after selectively reducing thoracic spine blood flow.¹³ Sarwahi also demonstrated using Laser Doppler flowmetry that spinal cord blood flow changes precede MEP loss at a mean of 15.8 minutes.⁴⁴ In that study, blood flow changes were induced by inflating a balloon in the epidural space. Our study induced blood flow changes in a more clinically applicable manner by studying spinal cord distraction. Changes in neurological (motor function) assessed by the Tarlov scale did not correlate with the change in blood flow or maximum distraction distance under the experimental parameters applied in these studies.

This study had a number of limitations. Among these are a relatively small population of sheep and the use of multiple probes to sample spatially separated sites in each sheep. We believe that although the sample size is small, this preliminary study demonstrates the ability of DCS to optically monitor spinal cord blood flow in a distraction model. Further rigorous animal and clinical studies will be needed to prove the real benefit of optical monitoring of the blood flow during spinal surgery. Previous work by the authors have shown that blood flow in the sheep spinal cord can reliably be detected using the DCS probe.^{29, 30} Thickness of the sheep skull limited our ability to obtain MEP data in all animals. We believe this does not disqualify our results as the measurements that we were able to obtain data showed reliable electrophysiological signals demonstrating the temporal relationship between decreased optical flow and decreased MEP amplitude. As this is a pilot study, future refinements in electrophysiologic technique will allow us to better study the relationship between blood flow and MEP signal change. The diffuse optical measurements we made were limited to relative changes in blood flow, which is a useful biomarker, but an incomplete metric of the adequacy of oxygen delivery to the tissue. Current intraoperative electrophysiological neuro-monitoring also uses relative

metrics, e.g., the monitoring alert corresponds to a relative decrease in amplitude from baseline measurements. We envision optical flow technology to be used in a similar way in that the relative change of blood flow from baseline measurements will be the clinically significant parameter. We also did not measure pure linear distraction because we did not disrupt the anterior and middle columns of the spine. Rather, an acute kyphotic deformity was created. Theoretically, this would stretch the dorsal sensory tracts more than the ventral motor tracts of the spinal cord. However, we believe our results are still valid and can be applied clinically, because pure distraction is a rare event and distraction often occurs with other deforming forces.

We envisage the initial applications of this novel technology during spinal surgical procedures where the spinal cord is at risk for ischemia, as a compliment to current electrophysiological techniques. While DCS systems are currently research tools and are currently not widely available nor typically designed for extended clinical use, there are several commercial devices addressing these challenges which have recently entered the market. The DCS probe can be inserted caudal to the operative levels either with a laminotomy or a small opening in the ligamentum flavum. In the current study, the spinal cord probe was easily inserted into the epidural space by creating a small laminotomy and blood flow signals were obtained in all animals. We have also previously placed these probes percutaneously. The probes can, like any epidural probe or catheter, occasionally cause venous bleeding within the epidural space. The probes at times required some optimization of positioning, through slight advancement, withdrawal, or rotation to optimize signal. A future probe design will have the ability to monitor multiple levels of the spinal cord via a single probe, throughout surgical procedures and continuously monitor blood flow. Any decrease in blood flow will be immediately apparent and allow the surgeon who can intervene to before neurologic injury ensues. A second application of this novel technique is to monitor ischemia in the setting of a traumatic spinal cord injury. In select individuals, the probe can be inserted percutaneously under fluoroscopic guidance, while in others the probe would be placed at the time of surgical intervention, providing the clinician with real time information regarding spinal cord perfusion intraoperatively, to guide stabilization, and perioperatively, to guide efforts at enhancing spinal cord flow.

Conclusions

In conclusion, in this pilot study we have demonstrated that our epidural fiber optic DCS device can detect a reduction in blood flow at the site of a distraction and can continuously and simultaneously monitor multiple sites along the spinal cord. Reduction in blood flow was found to temporally precede decrease in MEP amplitude and may therefore be of great value in providing an earlier warning of a potential problem to the surgeon during spinal surgery.

Acknowledgements

We thank Michael Mazzella, and K2M for graciously donating the spinal instrumentation used in this project. Prof. Rickson Mesquita, and Dr. Wesley Baker, provided valuable advice and suggestions. We also thank Kenneth Abramson, for his assistance with instrumentation and the veterinary staff of the Division of Laboratory Animal Resources at Stony Brook University.

References

1. Gallagher, M.J., Hogg, F.R.A., Zoumprouli, A., Papadopoulos, M.C. and Saadoun, S. (2019). Spinal Cord Blood Flow in Patients with Acute Spinal Cord Injuries. *J. Neurotrauma* 36, 919-929.
2. Squair, J.W., Belanger, L.M., Tsang, A., Ritchie, L., Mac-Thiong, J.M., Parent, S., Christie, S., Bailey, C., Dhall, S., Street, J., Ailon, T., Paquette, S., Dea, N., Fisher, C.G., Dvorak, M.F., West, C.R. and Kwon, B.K. (2017). Spinal cord perfusion pressure predicts neurologic recovery in acute spinal cord injury. *Neurology* 89, 1660-1667.
3. Martirosyan, N.L., Feuerstein, J.S., Theodore, N., Cavalcanti, D.D., Spetzler, R.F. and Preul, M.C. (2011). Blood supply and vascular reactivity of the spinal cord under normal and pathological conditions. *J. Neurosurg. Spine* 15, 238-251.
4. Dolan, E.J., Transfeldt, E.E., Tator, C.H., Simmons, E.H. and Hughes, K.F. (1980). The effect of spinal distraction on regional spinal cord blood flow in cats. *J. Neurosurg.* 53, 756-764.
5. Naito, M., Owen, J.H., Bridwell, K.H. and Sugioka, Y. (1992). Effects of distraction on physiologic integrity of the spinal cord, spinal cord blood flow, and clinical status. *Spine (Phila Pa 1976)* 17, 1154-1158.
6. Montalva-Iborra, A., Alcanyis-Alberola, M., Grao-Castellote, C., Torralba-Collados, F. and Giner-Pascual, M. (2017). Risk factors in iatrogenic spinal cord injury. *Spinal Cord* 55, 818-822.
7. Wu, D., Zheng, C., Wu, J., Xue, J., Huang, R., Wu, D. and Song, Y. (2017). The pathologic mechanisms underlying lumbar distraction spinal cord injury in rabbits. *Spine J* 17, 1665-1673.
8. Daniels, A.H., Hart, R.A., Hilibrand, A.S., Fish, D.E., Wang, J.C., Lord, E.L., Buser, Z., Tortolani, P.J., Stroh, D.A., Nassr, A., Currier, B.L., Sebastian, A.S., Arnold, P.M., Fehlings, M.G., Mroz, T.E. and Riew, K.D. (2017). Iatrogenic Spinal Cord Injury Resulting From Cervical Spine Surgery. *Global Spine J* 7, 84S-90S.

9. Owen, J.H., Naito, M. and Bridwell, K.H. (1990). Relationship among Level of Distraction, Evoked-Potentials, Spinal-Cord Ischemia and Integrity, and Clinical Status in Animals. *Spine (Phila Pa 1976)* 15, 852-857.
10. Shi, R. and Pryor, J.D. (2002). Pathological changes of isolated spinal cord axons in response to mechanical stretch. *Neuroscience* 110, 765-777.
11. Seyal, M. and Mull, B. (2002). Mechanisms of signal change during intraoperative somatosensory evoked potential monitoring of the spinal cord. *J. Clin. Neurophysiol.* 19, 409-415.
12. Devlin, V.J. and Schwartz, D.M. (2007). Intraoperative neurophysiologic monitoring during spinal surgery. *J. Am. Acad. Orthop. Surg.* 15, 549-560.
13. Lips, J., de Haan, P., Bouma, G.J., Jacobs, M.J. and Kalkman, C.J. (2002). Delayed detection of motor pathway dysfunction after selective reduction of thoracic spinal cord blood flow in pigs. *J. Thorac. Cardiovasc. Surg.* 123, 531-538.
14. Nielsen, V.K. and Kardel, T. (1981). Temporospacial effects on orthodromic sensory potential propagation during ischemia. *Ann. Neurol.* 9, 597-604.
15. Deiner, S. (2010). Highlights of anesthetic considerations for intraoperative neuromonitoring. *Semin. Cardiothorac. Vasc. Anesth.* 14, 51-53.
16. Wang, A.C., Than, K.D., Etame, A.B., La Marca, F. and Park, P. (2009). Impact of anesthesia on transcranial electric motor evoked potential monitoring during spine surgery: a review of the literature. *Neurosurg. Focus* 27, E7.
17. Nuwer, M.R., Emerson, R.G., Galloway, G., Legatt, A.D., Lopez, J., Minahan, R., Yamada, T., Goodin, D.S., Armon, C., Chaudhry, V., Gronseth, G.S., Harden, C.L., Therapeutics, Technology Assessment Subcommittee of the American Academy of, N. and American Clinical Neurophysiology, S. (2012). Evidence-based guideline update: intraoperative spinal monitoring with somatosensory and transcranial electrical motor evoked potentials: report of the Therapeutics and Technology Assessment Subcommittee of the American Academy of Neurology and the American Clinical Neurophysiology Society. *Neurology* 78, 585-589.

18. Lindsberg, P.J., Jacobs, T.P., Frerichs, K.U., Hallenbeck, J.M. and Feuerstein, G.Z. (1992). Laser-Doppler flowmetry in monitoring regulation of rapid microcirculatory changes in spinal cord. *Am. J. Physiol.* 263, H285-292.
19. Simonovich, M., Barbiro-Michaely, E. and Mayevsky, A. (2008). Real-time monitoring of mitochondrial NADH and microcirculatory blood flow in the spinal cord. *Spine (Phila Pa 1976)* 33, 2495-2502.
20. Hamamoto, Y., Ogata, T., Morino, T., Hino, M. and Yamamoto, H. (2007). Real-time direct measurement of spinal cord blood flow at the site of compression: relationship between blood flow recovery and motor deficiency in spinal cord injury. *Spine (Phila Pa 1976)* 32, 1955-1962.
21. Jacques, S.L. (2013). Optical properties of biological tissues: a review. *Phys. Med. Biol.* 58, R37-61.
22. Boas, D.A. and Yodh, A.G. (1997). Spatially varying dynamical properties of turbid media probed with diffusing temporal light correlation. *Journal of the Optical Society of America A-Optics Image Science and Vision* 14, 192-215.
23. Durduran, T., Choe, R., Baker, W.B. and Yodh, A.G. (2010). Diffuse Optics for Tissue Monitoring and Tomography. *Rep Prog Phys* 73, 076701.
24. Yu, G., Floyd, T.F., Durduran, T., Zhou, C., Wang, J., Detre, J.A. and Yodh, A.G. (2007). Validation of diffuse correlation spectroscopy for muscle blood flow with concurrent arterial spin labeled perfusion MRI. *Opt. Express* 15, 1064-1075.
25. Carp, S.A., Dai, G.P., Boas, D.A., Franceschini, M.A. and Kim, Y.R. (2010). Validation of diffuse correlation spectroscopy measurements of rodent cerebral blood flow with simultaneous arterial spin labeling MRI; towards MRI-optical continuous cerebral metabolic monitoring. *Biomed Opt Express* 1, 553-565.

26. Buckley, E.M., Hance, D., Pawlowski, T., Lynch, J., Wilson, F.B., Mesquita, R.C., Durduran, T., Diaz, L.K., Putt, M.E., Licht, D.J., Fogel, M.A. and Yodh, A.G. (2012). Validation of diffuse correlation spectroscopic measurement of cerebral blood flow using phase-encoded velocity mapping magnetic resonance imaging. *J. Biomed. Opt.* 17, 037007.
27. Zhou, C., Eucker, S.A., Durduran, T., Yu, G., Ralston, J., Friess, S.H., Ichord, R.N., Margulies, S.S. and Yodh, A.G. (2009). Diffuse optical monitoring of hemodynamic changes in piglet brain with closed head injury. *J. Biomed. Opt.* 14, 034015.
28. Buckley, E.M., Cook, N.M., Durduran, T., Kim, M.N., Zhou, C., Choe, R., Yu, G., Schultz, S., Sehgal, C.M., Licht, D.J., Arger, P.H., Putt, M.E., Hurt, H.H. and Yodh, A.G. (2009). Cerebral hemodynamics in preterm infants during positional intervention measured with diffuse correlation spectroscopy and transcranial Doppler ultrasound. *Opt. Express* 17, 12571-12581.
29. Mesquita, R.C., D'Souza, A., Bilfinger, T.V., Galler, R.M., Emanuel, A., Schenkel, S.S., Yodh, A.G. and Floyd, T.F. (2013). Optical monitoring and detection of spinal cord ischemia. *PLoS One* 8, e83370.
30. Kogler, A.S., Bilfinger, T.V., Galler, R.M., Mesquita, R.C., Cutrone, M., Schenkel, S.S., Yodh, A.G. and Floyd, T.F. (2015). Fiber-optic Monitoring of Spinal Cord Hemodynamics in Experimental Aortic Occlusion. *Anesth.* 123, 1362-1373.
31. Sheng, S.R., Wang, X.Y., Xu, H.Z., Zhu, G.Q. and Zhou, Y.F. (2010). Anatomy of large animal spines and its comparison to the human spine: a systematic review. *Eur. Spine J.* 19, 46-56.
32. Rose, F.X., Estebe, J.P., Ratajczak, M., Wodey, E., Chevanne, F., Dollo, G., Bec, D., Malinovsky, J.M., Ecoffey, C. and Le Corre, P. (2007). Epidural, intrathecal pharmacokinetics, and intrathecal bioavailability of ropivacaine. *Anesth. Analg.* 105, 859-867.
33. Daudel, F., Bone, H.G., Traber, D.L., Stubbe, H.D., Lettau, M., Lange, M., Scharte, M., Van Aken, H. and Westphal, M. (2006). Effects of thoracic epidural anesthesia on hemodynamics and global oxygen transport in ovine endotoxemia. *Shock* 26, 615-619.

34. Bockler, D., Kotelis, D., Kohlhof, P., von Tengg-Kobligk, H., Mansmann, U., Zink, W., Horner, C., Ortlepp, I., Habel, A., Kauczor, H.U., Graf, B. and Allenberg, J.R. (2007). Spinal cord ischemia after endovascular repair of the descending thoracic aorta in a sheep model. *Eur. J. Vasc. Endovasc. Surg.* 34, 461-469.
35. Lehr, E.J., Coe, J.Y. and Ross, D.B. (2007). An intra-aortic shunt prevents paralysis during aortic surgery in sheep. *J. Surg. Res.* 141, 78-82.
36. Lin, W., Busch, D.R., Goh, C.C., Barsi, J. and Floyd, T.F. (2019). Diffuse Correlation Spectroscopy Analysis Implemented on a Field Programmable Gate Array. *IEEE Access* 7, 122503-122512.
37. Tarlov, I.M. (1957). Spinal cord compression: mechanism of paralysis and treatment. Thomas.
38. Popovich, P.G., Tovar, C.A., Wei, P., Fisher, L., Jakeman, L.B. and Basso, D.M. (2012). A reassessment of a classic neuroprotective combination therapy for spinal cord injured rats: LPS/pregnenolone/indomethacin. *Exp. Neurol.* 233, 677-685.
39. LeBlanc, A.C., Kovacs, D.M., Chen, H.Y., Villare, F., Tykocinski, M., Autilio-Gambetti, L. and Gambetti, P. (1992). Role of amyloid precursor protein (APP): study with antisense transfection of human neuroblastoma cells. *J. Neurosci. Res.* 31, 635-645.
40. Otsuka, N., Tomonaga, M. and Ikeda, K. (1991). Rapid appearance of beta-amyloid precursor protein immunoreactivity in damaged axons and reactive glial cells in rat brain following needle stab injury. *Brain Res.* 568, 335-338.
41. Hortobagyi, T., Wise, S., Hunt, N., Cary, N., Djurovic, V., Fegan-Earl, A., Shorrock, K., Rouse, D. and Al-Sarraj, S. (2007). Traumatic axonal damage in the brain can be detected using β -APP immunohistochemistry within 35 min after head injury to human adults. *Neuropathol. Appl. Neurobiol.* 33, 226-237.
42. Geddes, J.F., Whitwell, H.L. and Graham, D.I. (2000). Traumatic axonal injury: practical issues for diagnosis in medicolegal cases. *Neuropathol. Appl. Neurobiol.* 26, 105-116.

43. Hong, J.Y., Suh, S.W., Lee, S.H., Park, J.H., Park, S.Y., Rhyu, I.J. and Yang, J.H. (2016). Continuous distraction-induced delayed spinal cord injury on motor-evoked potentials and histological changes of spinal cord in a porcine model. *Spinal Cord* 54, 649-655.

44. Sarwahi, V., Galina, J., Hasan, S., Thornhill, B., Legatt, A., Pawar, A., Moguevich, M. and Amaral, T.D.J.S. (2019). A Study of Critical Events That Lead to Spinal Cord Injury and the Importance of Rapid Reversal of Surgical Steps in Improving Neurological Outcomes: A Porcine Model.

Table 1: Summary of probe positions, distraction sites, maximum changes in distraction (mm), minimum relative blood flow (Δ BF, %) and β -APP score caudal to, at, and cranial to the site of distraction. Δ BF was averaged over the 10 minute period of maximum distraction. Up to 3 probes were placed with up to two adjacent positions recorded per probe. Not all sites were measured for each sheep; sites without measurements are designated by NA; the average is reported for sites with two measurements. Sheep 1 expired during recovery and was not included in histopathological analysis.

Sheep	Distraction location			Distraction Max. [mm]	Distraction Caudal	Δ BF [%]			β -APP		
	Caudal	At site	Cranial			At site	Cranial	Caudal	At site	Cranial	
1	NA	T9/10	NA	25	NA	-43	NA	NA	NA	NA	NA
2	NA	T13/1 4	NA	8	NA	-37	NA	1	34	1	1
3	NA	T13	T9/10	25	NA	-43	-10	1	58	1	1
4	T13/L1	T12/1 3	T10/1 1	25	-9	-43	34	15	42	0	0
5	NA	T13/L 1	T11/1 2	8	NA	-33	6	75	0	100	100
6	NA	T13/L 1	T12/1 3	21	NA	-55	-18	60	100	0	0
7	NA	T12/1 3	T11/1 2	19	NA	-43	-4	24	6	1	1
8	NA	L1/T1 3	T11/1 2	13	NA	-20	-10	0	1	0	0
9	L1/2	T12/1	T11/1	27	-41	-24	-31	40	38	1	1

		3	2							27
10	L1/2	T12/1	T8/9	29	8	-19	43	0	80	70
		3								
			Medi	23	-9	-40	-7	15	38	1
			an:							

Figure 1

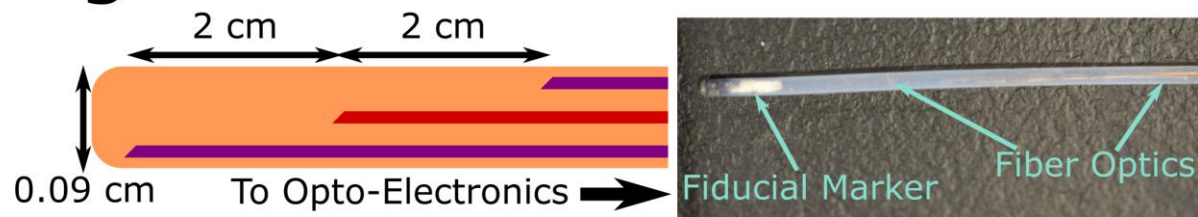


Figure 1

Schematic and photo of the distal tip of the fiber optic probe. Tissue is interrogated roughly $1/3 \pm 1/3$ of the source-detector separation; thus, the current configuration of the probe allows for measurement of blood flow throughout most of the spinal cord (cross-section approximately 1 cm). Det = DCS detector fiber; Src = DCS source fiber.

Figure 2

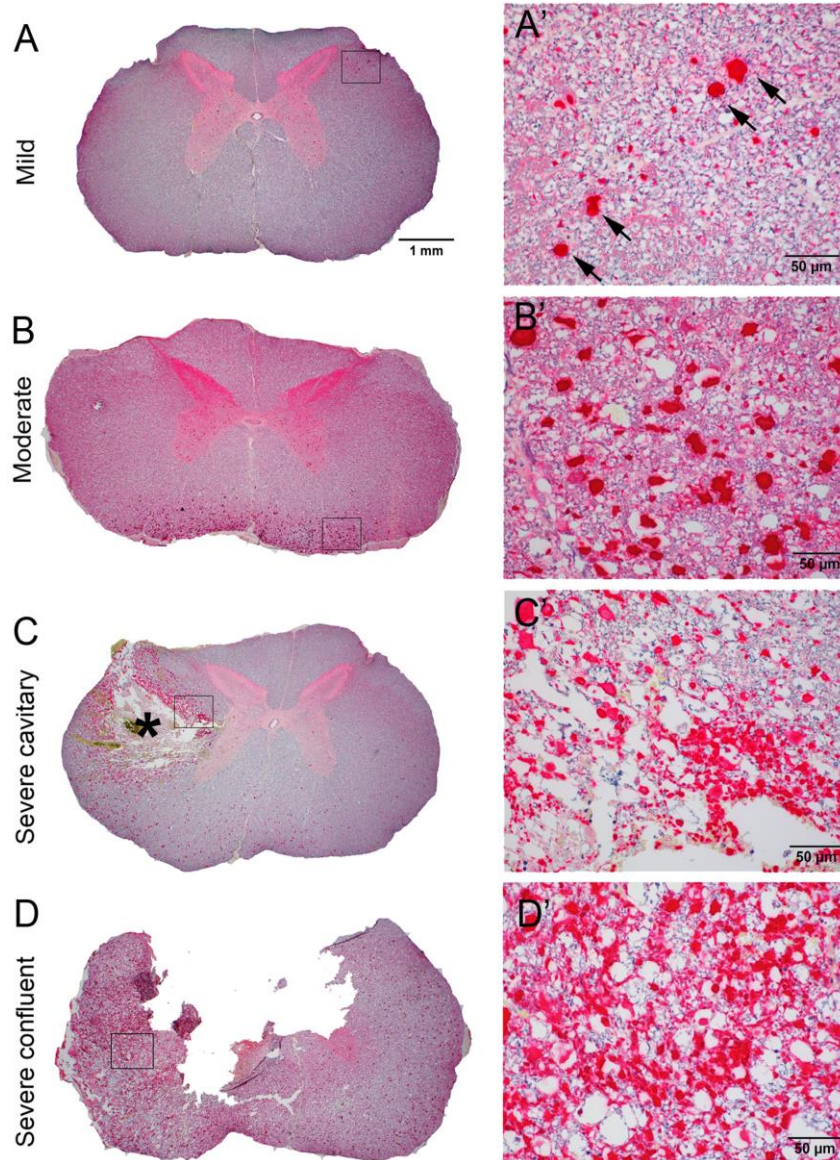


Figure 2

Quantitative scoring of spinal cord injury by β -APP immunohistochemical staining. (A, B, C, D): low magnification (2x) image of complete spinal cord cross section. The boxed area indicates the region of highest spheroid density. (A', B', C', D'): high magnification (40x) image from the corresponding boxed area. The β -APP score was generated by counting the number of spheroids with diameter $>10 \mu\text{m}$ (A' arrows) per 40x HPF in the highest region. (A, A'): Mild injury. (B, B'): Moderate injury. (C, C'): Severe injury with cavity (*) and hemorrhage. (D, D') Severe injury with confluent β -APP staining.

Figure 3

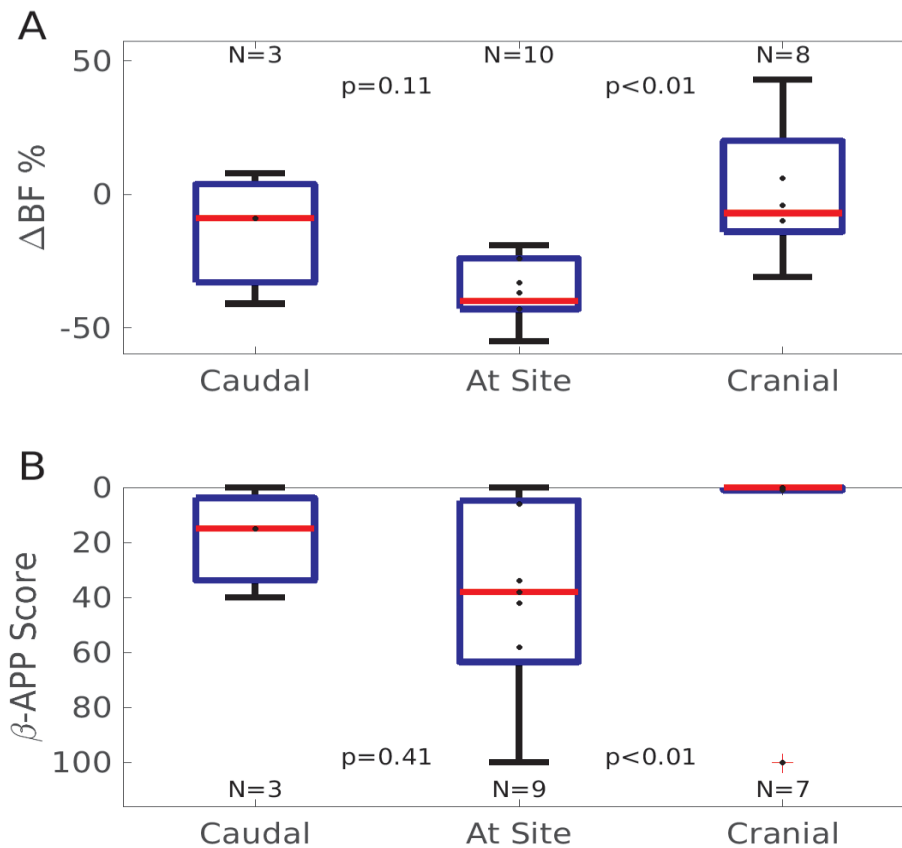


Figure 3

(A) change in blood flow from baseline and (B) β -APP score caudal to, at, and cranial to the site of distraction in 10 sheep. The number of measurements at each spatial location varied and is noted above each group. In three sheep, blood flow was measured caudal to the site of injury; in eight sheep, blood flow was measured cranial to the site of injury (three sheep had measurements both cranial and caudal to the distraction site). Neither the β -APP score nor blood flow was different between the sites caudal to and at the injury (Wilcoxon's signed-rank test). However, Δ BF significantly ($p < 0.01$) and β -APP nearly significantly ($p = 0.051$) differed between the site of injury and locations in the spinal cord cranial to the injury. Median Δ BF caudal to site -9 (IQR [-25, -1]), at site -40 [-43, -26], and cranial to site -7 [-12, 13]. Median β -APP score caudal to site 15 [4, 34], at site 38 [5, 64], and cranial to site 0 [0, 1]. Sheep 1 was excluded from the β -APP measurements because it died during extubation. The sample from Sheep 10 cranial to the site of distraction was damaged and no β -APP score was calculated.

Figure 4

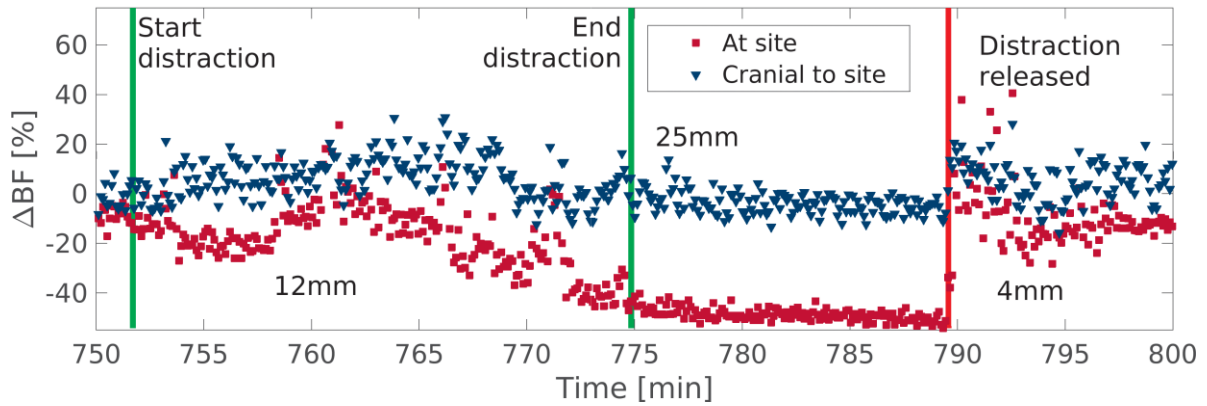


Figure 4

An example of temporal blood flow monitoring at two different locations on the spine (sheep 3). The green vertical lines denote the start and stop of increasing distraction; the red vertical line denotes the release of distraction. Distances (12 mm, 25 mm, and 4 mm) are changes from baseline at mid-distraction, maximal distraction, and after distraction was released, respectively. The spine did not fully relax into its pre-distraction position after release of mechanical distraction (4 mm from baseline position).

Figure 5

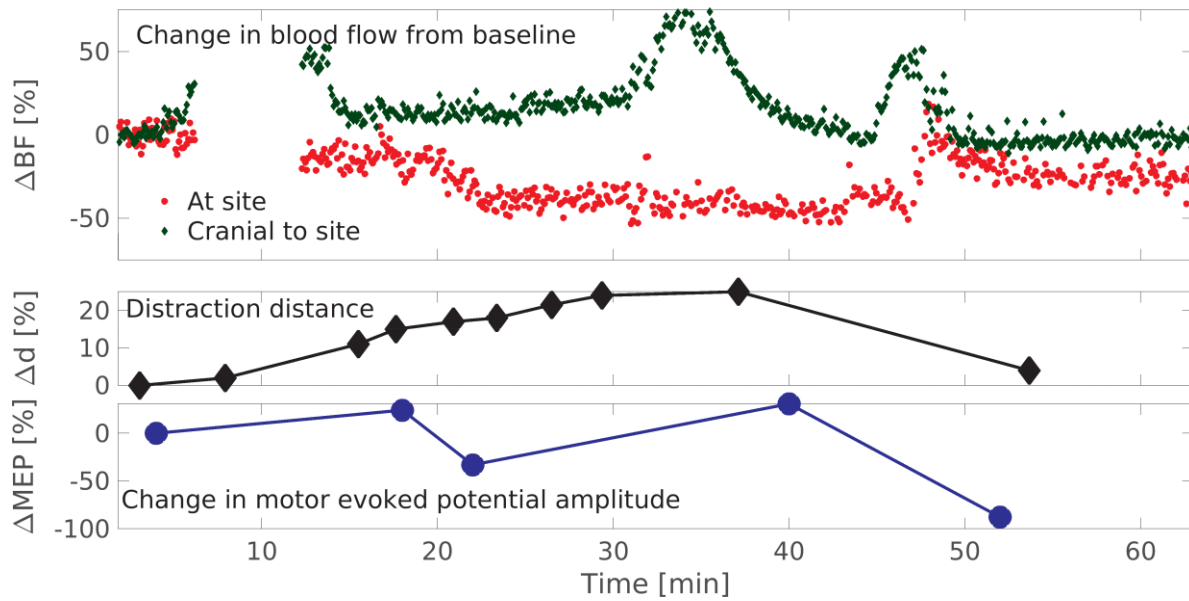


Figure 5

Temporal changes in relative blood flow (ΔBF), distraction distance (Δd), and MEP amplitude (ΔMEP) in Sheep 4. There was a persistently high (minimum 33% of baseline) MEP amplitude during distraction, despite declines in blood flow ($\Delta BF = 50\%$) for 20 minutes.

Figure 6

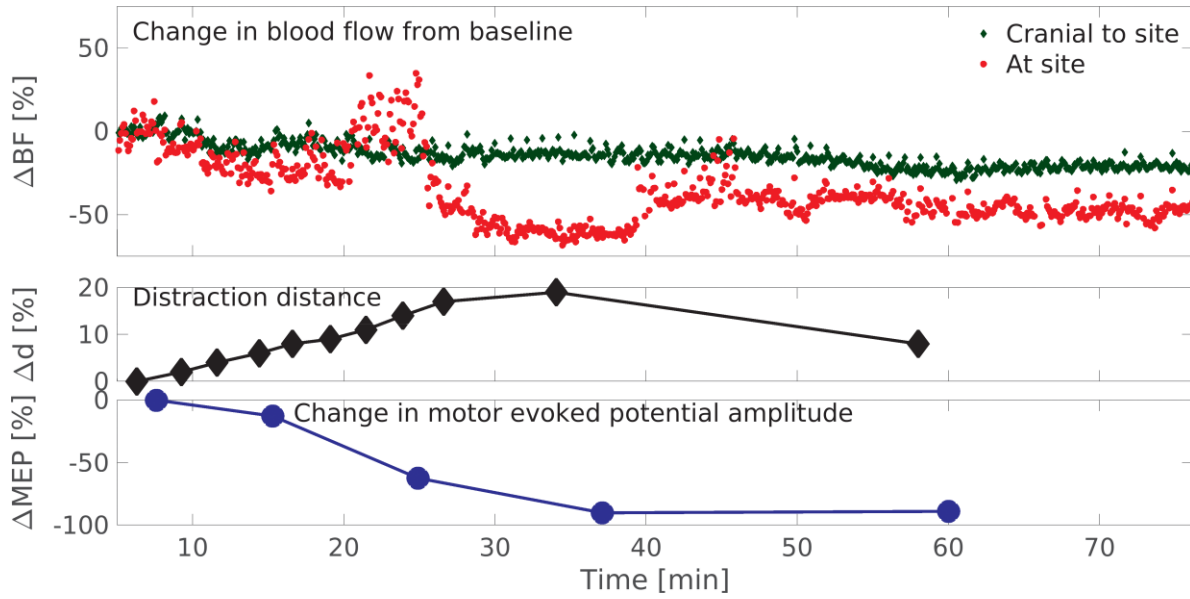


Figure 6

Temporal changes in relative blood flow (ΔBF), distraction distance (Δd), and MEP amplitude (ΔMEP) in Sheep 7. In this animal, the MEP amplitude more closely tracked the blood flow as a function of time.